Evidence of Ion Transport through Surface Conduction in Alkylsilane-Functionalized Nanoporous Ceramic Membranes

Anthony Y. Ku,* James A. Ruud, Thomas A. Early, and Reed R. Corderman

General Electric, Global Research Center, 1 Research Circle, Niskayuna, New York 12309

Received May 31, 2006. In Final Form: July 21, 2006

Alkylsilane-modified nanoporous ceramic membranes exclude water from their pores yet exhibit transmembrane electrical conductivity in aqueous electrolyte solutions. That effect was studied using impedance spectroscopy and ^{29}Si NMR. Anodic aluminum oxide membranes with alkylsilane-functionalized pores exhibited a transmembrane electrical resistance that increased with the length of the hydrocarbon chain. Microstructural studies revealed that the conduction was due primarily to a small number of "hydrophilically defective" pores in membranes modified by long-chain alkylsilanes and both hydrophilic defects *and* surface conduction in pores modified by short-chain alkylsilanes. Hydroxyl groups in short-chain alkylsilane layers act as "water wires" to enable surface ion transport. The local concentration of hydroxyl groups decreased with alkylsilane chain length, explaining the resistance trend. This constitutes the first direct evidence that alkylsilane functionalization affects electrical as well as wetting properties.

Introduction

Chemical modification using organosilanes is an effective and flexible method for engineering the wetting and adsorption properties of a ceramic surface.[1] One example is the use of alkylsilanes to render a surface hydrophobic. The uniformity and stability of the surface modification are extremely sensitive to the structure of the coating, which depends on the details of the alkylsilane chemistry and the functionalization conditions.[2−4] Consequently, a great deal of effort has been expended in understanding the relationship among processing, structure, and properties. This has enabled a number of emerging technologies in the areas of microfluidics and biosensing.[5−13]

The modification of a surface with alkylsilanes impacts more than the wetting properties. Recently, there has been evidence that the electrical properties are also affected. Steinle et al. reported that alkylsilane-modified alumina membranes mimic the behavior of ion channels and can be used to detect amphiphilic biomolecules.[8] They found that the electrical resistance across an octadecylsilane-modified anodic aluminum oxide (AAO) membrane immersed in an aqueous electrolyte solution was initially very high ($\sim$4 M$\Omega\cdot$cm^2) but decreased by 4 orders of magnitude as the concentration of amphiphilic molecules increased. It was hypothesized that the silane treatment rendered the pores hydrophobic and that the amphiphilic biomolecules partitioned into the silane structure and allowed electrolyte to flood the pores, causing the drop in resistance. However, no explanation for the initial conductivity was provided.

Although this initial resistance was high, it is still lower than the $\sim 1 \times 10^4$ M$\Omega\cdot$cm^2 that would be expected for if the alumina pores were filled with air. An even higher resistance ($> 1 \times 10^7$ M$\Omega\cdot$cm^2) would be expected if the pores were completely filled with octadecane.[14] This letter examines the possibility that ionic conduction occurs as a result of surface transport within the alkylsilane layer. Three sets of experiments were performed to test this hypothesis. First, the electrical behavior of a series of alkylsilane-modified alumina membranes with different hydrocarbon chain lengths was measured using impedance spectroscopy in order to determine the effect of alkyl group length on membrane conductivity. Second, electrodeposition experiments were performed using alkylsilane-modified AAO substrates to determine the extent of electrolyte penetration into the hydrophobic pores and estimate its contribution to the total ionic transport. Finally, the microstructure of the modified alumina surface was characterized using ^{29}Si NMR to resolve the relative abundance of Si−O−Si cross links, Si−OAl surface grafts, and Si−OH silanols. Evidence will be presented for the structural features in the silane layer that can result in surface ionic conduction.

Experimental Section

Sample Preparation. *Materials.* Experiments were performed using commercial Anopore AAO membranes (Whatman, 200 nm pores, 60 μm thick) and PTFE membranes (Pall, 200 nm pores). Alkyltrichlorosilanes with tail lengths of C_1 to C_{18}, toluene, 1,1,1,3,3,3-hexamethyldisilazane (HMDZ), and potassium chloride (KCl) were purchased from Aldrich and used as received. Poly(dimethylsiloxane) (Sylgard 184, Dupont) was obtained from Robert McKeown Co. (Branchburg, NJ).

Surface Functionalization. Prior to functionalization, AAO membranes were heated in air at 550 °C for 4 h, immersed in 30% H_2O_2 for 45 min at room temperature, transferred to boiling water for 30 min, and dried at 80 °C in air for 1 h. In a typical experiment, 40 mL of dry toluene was added to a 100 mL round-bottomed flask under flowing argon, followed by a quantity of alkylsilane to produce a 0.076 M solution. The AAO was added under flowing nitrogen. After 24 h, the samples were thoroughly rinsed with toluene to remove unreacted alkylsilane and dried in air at 80 °C for 1 h.

* Corresponding author. E-mail: kua@research.ge.com. Tel: (01)-518-387-4628. Fax: (01)-518-387-7563.

(1) Wasserman, S. R.; Tao, Y.-T.; Whitesides, G. M. *Langmuir* **1989**, *5*, 1074−1087.
(2) Angst, D. L.; Simmons, G. W. *Langmuir* **1991**, *7*, 2236−2242.
(3) Fadeev, A. Y.; McCarthy, T. J. *Langmuir* **2000**, *16*, 7268−7274.
(4) Takei, T.; Yamazaki, A.; Watanabe, T.; Chikazawa, M. *J. Colloid Interface Sci.* **1997**, *188*, 409−414.
(5) Zhao, B.; Moore, J. S.; Beebe, D. J. *Science* **2001**, *291*, 1023−1026.
(6) Cornell, B. A.; Braach-Maksvytis, V. L. B.; King, L. G.; Osman, P. D. J.; Rause, B.; Wieczorek, L.; Pace, R. J. *Nature* **1997**, *387*, 580−583.
(7) Srinivasan, U.; Houston, M. R.; Howe, R. T. *J. Microelectromech. Syst.* **1998**, *7*, 252−260.
(8) Steinle, E. D.; Mitchell, D. T.; Wirtz, M.; Lee, S. B.; Young, V. Y.; Martin, C. R. *Anal. Chem.* **2002**, *74*, 2416.
(9) Caro, J.; Noack, M.; Kölsch, P. *Microporous Mesoporous Mater.* **1998**, *22*, 321.
(10) Singh, R. P.; Way, J. D.; Dec, S. F. *J. Membr. Sci.* **2005**, *259*, 34−46.
(11) McCarley, K. C.; Way, J. D. *Sep. Purif. Technol.* **2001**, *25*, 195.
(12) Nishiyama, N.; Park, D.-H.; Egashira, Y.; Ueyama, K. *Sep. Purif. Technol.* **2003**, *32*, 127.
(13) Sah, A.; Castricum, H. L.; Bliek, A.; Blank, D. H. A.; ten Elshof, J. E. *J. Membr. Sci.* **2004**, *243*, 125.
(14) Noble, I. E.; Taylor, D. M. *J. Phys D: Appl. Phys.* **1980**, 2115.

10.1021/la0615591 CCC: $33.50
Published on Web 08/26/2006

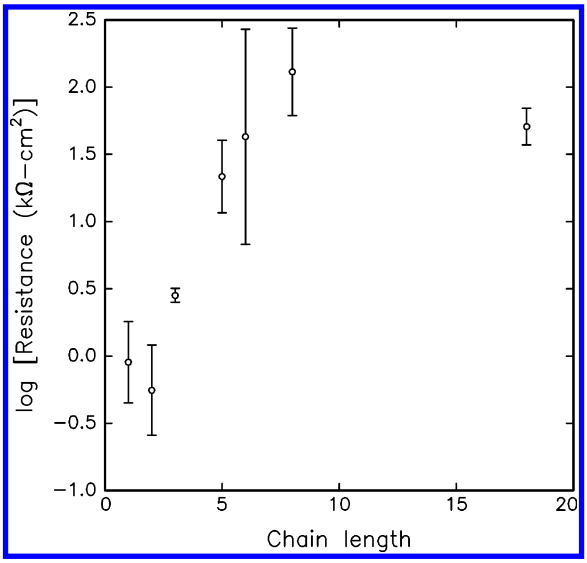

Figure 1. Area-specific resistance of AAO membranes treated with trichloroalkylsilanes with alkyl tail lengths up to C_{18}. The log of the membrane resistance is plotted against tail length. For each alkyl tail length, three measurements were collected on each of the three samples. The electrolyte solution was 0.1 M KCl.

Mounting. The membranes were mounted between two PTFE washers using PDMS to provide mechanical stability during testing. The exposed aperture area was 0.32 cm^2.

Electrodeposition Experiments. To probe for the presence of aqueous electrolytes in the hydrophobically modified pores, platinum was electrodeposited in AAO (1.3 μm thick) supported on a conducting substrate. Details of the substrate preparation and electrodeposition are included in the Supporting Information. Prior to electrodeposition, the substrates were immersed for 1 h in 10 mM alkyltrichlorosilane (C_1 or C_{18}) solution in dry toluene. After electrodeposition, each substrate was rinsed with toluene, dried, and examined by scanning electron microscopy (SEM).

Sample Characterization. *Electrical Impedance.* Four-wire, two-electrode ac impedance measurements were performed with a Solartron model 1480 potentiostat and a model 1260 frequency analyzer. The frequency was 0.1 to 10^7 Hz, and the signal amplitude was 10 mV. Three measurements were taken on three samples for each chain length. Measurements were performed in custom-built polycarbonate test cells with Pt mesh (Alfa Aesar, 52 mesh woven from 0.1-mm-diameter wire) electrodes. The membrane was clamped between the half-cells, electrolyte (0.1 M KCl) was added, and the interface was agitated to remove air bubbles. Prior to testing, the membranes were soaked in distilled water for 3 h to ensure good fluid contact with the pores. The electrical resistance was taken as the Z' intercept on the Nyquist plot. The membrane resistance was determined by correcting for the cell resistance, which closely matched the expected resistance of 0.1 M KCl in the testing geometry.

^{29}Si NMR. Cross-polarization magic angle spinning (CPMAS) NMR was used to analyze C_1- and C_{18}-treated AAO. Sample membranes were crushed into a fine powder. HMDZ-treated C_1-treated AAO samples were prepared by immersing 1.35 g of crushed C_1-treated AAO in 2.5 mL of HMDZ for 15 min. HMDZ-treated C_{18}-treated AAO powder was prepared in a similar manner. The sample was then rinsed with toluene and dried at 80 °C for 1 h. All spectra were obtained on a Bruker Avance 300 MHz instrument in a 7 mm rotor spinning at 6.000 kHz. Scans (200 000) were accumulated for each spectrum using the standard cross-polarization pulse sequence with a cross-polarization contact time of 4 ms and a repetition time of 2 s.

Results

Figure 1 shows the electrical resistance of a series of membranes functionalized with alkyltrichlorosilanes of tail chain length ranging from C_1 to C_{18}. The log of the resistance is plotted as a function of the alkyl tail chain length. Upon alkylsilane functionalization, the resistance increased about 3 orders of magnitude from 0.1 kΩ·cm^2 for an untreated AAO control. The resistance trended upward with increasing tail length, with the rate of increase gradually leveling off at an area specific resistance of 50 kΩ·cm^2 for C_{18}-treated AAO. A fully hydrophobic PTFE membrane with comparable porosity exhibited open circuit behavior on the Nyquist plot. Given the instrument capability, this corresponded to a resistance in excess of 300 MΩ·cm^2.

To determine the extent of aqueous electrolyte penetration in the hydrophobically modified pores, platinum was electrodeposited in functionalized AAO supported on conducting substrates. The presence of platinum in a pore was taken as evidence that electrolyte penetrated the pore. Cross-sectional SEM imaging revealed platinum in a minority of the pores with deposition rates of 0.0023 (1 in 430 pores) and 0.0043 (1 in 232 pores) for the C_1- and C_{18}-treated AAO, respectively. To determine if these "hydrophilically defective" pores could completely explain the observed electrical behavior, the effective resistance of the membrane was computed assuming a bimodal population of completely wetted and completely dry pores. Assuming that ion transport occurs only through hydrophilically defective pores, the measured defect rates correspond to resistances of about 20 and 11 kΩ·cm^2 for C_1- and C_{18}-treated membranes. These values correspond to upper bounds on the defect rate and lower limits on the resistance because the AAO used for electrodeposition was thinner than the AAO used for the impedance measurements (1.3 vs 60 μm).[15]

For the C_{18} case, the measured resistance (50 vs 11 kΩ·cm^2) was higher by about half an order of magnitude than the lower bound. This suggests that the thicker AAO used for the impedance measurement did indeed have a lower defect rate than the AAO used for the electrodeposition experiment. In contrast, the measured resistance for the C_1 case (5.5 vs 20 kΩ·cm^2) was about half an order of magnitude too low. This indicates that the measured behavior cannot be explained *solely* by the presence of hydrophilically defective pores and that a second mechanism is operative in membranes functionalized with shorter alkylsilane chains.

^{29}Si CPMAS NMR was used to resolve the molecular interconnections between silicon atoms within the alkylsilane layers, providing direct information about the microstructure and insight into this second mechanism. A similar approach was used by Singh to study the hydroxyl content and degree of cross-linking in C_{18}-modified Vycor substrates.[10] This study focused on peaks corresponding to trifunctional T groups in C_1- and C_{18}-modified AAO. Three types of T groups were present: (i) T, with all three oxygens connected to neighboring silicon atoms, (ii) T-OH, with one of the neighboring oxygen−silicon linkages replaced by a hydroxyl group, and (iii) T-OAl, with one of the oxygen−silicon linkages replaced by an oxygen−aluminum bond to the alumina surface.

Figure 2 shows two sets of ^{29}Si NMR spectra corresponding to C_1- and C_{18}-modified samples. For each set, data are shown *before* and *after* reaction with HMDZ. The high-field peak at −68 ppm corresponds to the trifunctional T whereas the low-field peak at −59 ppm contains contributions from both T-OH

(15) A pore must be hydrophilically defective along its entire length in order to accommodate ion transport or electrodeposition. Because of the need to ensure good electrical contact for electrodeposition, the AAO used for the Pt deposition experiments was much thinner (1.3 μm) than the AAO used for impedance measurements (60 μm). Because the alkylsilane structure in longer pores would be less likely to be hydrophilically defective along its the *entire* length than a shorter pore, the defect rates measured from the Pt electrodeposition experiments represent upper limits. Because the resistance varies inversely with the defect rate, the estimated resistances are lower bounds.

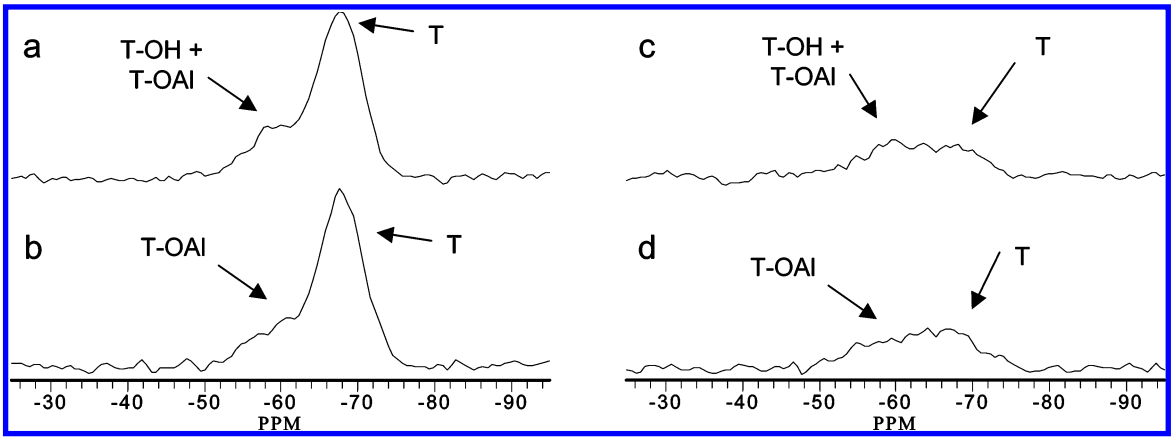

Figure 2. ^{29}Si CPMAS NMR spectra for alkysilane-treated AAO. Spectra are shown for (a) C_1-treated AAO, (b) C_1-treated, HMDZ-treated AAO, (c) C_{18}-treated AAO, and (d) C_{18}-treated, HMDZ-treated AAO. The T, T-OH, and T-OAl peaks are labeled on each spectrum.

Table 1. Integrated Area[a]

	C_1	C_1 + HMDZ	C_{18}	C_{18} + HMDZ
low-field (T-OH and/or T-OAl)	41	29	29	24
high-field (T)	86	83	15	16
total Si signal	128	112	43	40
low/high	0.48	0.35	2.0	1.5

[a] Arbitrary units.

and T-OAl. The relative contributions from T-OH and T-OAl were separated by treating the sample with HMDZ, which reacts with exposed silanols in T-OH to form M groups at about +9 ppm (not shown). The residual low-field peak after HMDZ treatment was attributed to T-OAl as well as T-OH silanols that were not accessible to the HMDZ.

Two qualitative features are evident. First, the signal from C_1-treated samples is stronger than the signal from C_{18}-treated samples, particularly for the high-field T peak. This is not surprising, given the known tendency of small alkylsilane molecules to cross react to form siloxane networks.[3] Second, the low-field peak decreases in intensity relative to the high-field peak after HMDZ treatment. This indicates the presence of accessible silanol groups in both the C_1- and C_{18}-treated samples, which was expected because T-based siloxane structures almost always contain some residual unreacted silanols.[2]

The peak intensities were determined using a custom application that deconvoluted each of the four spectra simultaneously using two lines. The shape, width, and chemical shift of each of the two lines were constrained to be independent from one another but the same from spectrum to spectrum. The intensity of the two lines was optimized independently in each of the four spectra. The integrated areas of each peak were normalized by the weight of the sample used in the NMR spectra. Table 1 lists the integrated intensities of the high- and low-field peaks in each spectrum. The total integrated area of the two lines shows that the as-prepared C_1-treated sample contained three times as much silicon as the C_{18}-treated sample and the C_{18}-treated sample loses twice as many hydroxyls upon HMDZ treatment. On the basis of the standard error of the deconvolution, these quantitative metrics are just at the limit of observation.

Discussion

Figure 3 shows schematics of three microstructures that can be produced by alkylsilanes: a perfect monolayer, a lightly cross-linked multilayer, and a heavily cross-linked multilayer. Perfect monolayers contain neither T nor T-OH groups and would be expected to exhibit high electrical resistance because of the

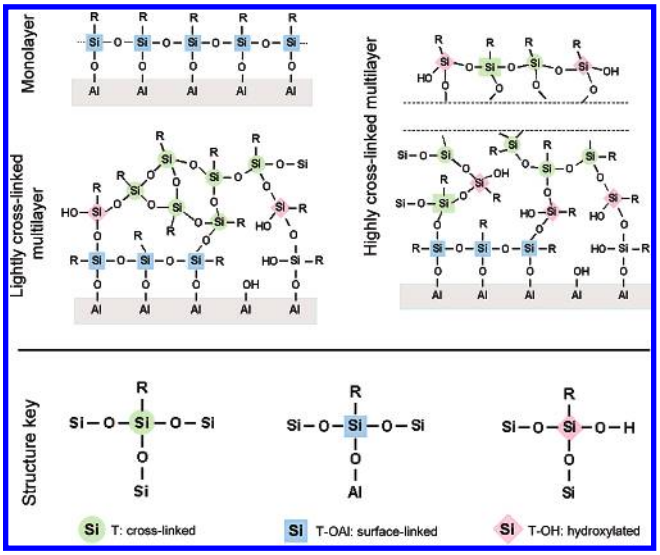

Figure 3. Alkylsilane microstructures corresponding to T, T-OH, and T-OAl groups. Alkylsilanes can form perfect monolayers, thin, lightly cross-linked multilayers, and thick, highly cross-linked multilayers. Only T-OAl groups are expected for perfect monolayers. In cross-linked structures, T, T-OH, and T-OAl groups are present.

deficiency of hydroxyl groups. However, cross-linked multilayers possess all three types of T groups. Thin, lightly cross-linked multilayers form from C_{18} alkylsilanes. The steric hindrance resulting from the long hydrocarbon tails prevents extensive cross linking. In contrast, the smaller C_1 alkylsilanes cross react readily, leading to thick, highly cross-linked multilayers. In both cases, the presence of T-OH groups provides a polar environment within the siloxane network, allowing a path for ion transport. The total amount of T-OH would be higher in the thicker C_1 layer. Although the NMR data indicate a highly cross-linked C_1 siloxane network, there was no discernible difference in the air permeability of the C_1- and C_{18}-treated samples. This indicates that both the C_1 and C_{18} multilayers are thin (<5 nm) relative to the diameter of the AAO pore. (See Supporting Information for additional details.)

The systematic increase in impedance between C_1 and C_6 alkylsilane-treated membranes (Figure 1) could result from a decrease in the level of cross linking as the steric hindrance increased with increasing chain length. Between C_6 and C_{18}, the amount of cross linking is presumably similar when the impedance is similar. That is in close agreement with observations that self-assembled monolayers of OTS on silicon surfaces were observed to transition from oligomeric to monomeric structures at C_6 tail lengths.[3] Moreover, given the results of the electrodeposition experiments, it is plausible that the hydrophilic

defects are the dominant mechanism of ionic transport in membranes functionalized with longer tail lengths. In shorter-chain samples, the measured resistance is lower than would be expected if hydrophilic defects are solely responsible for the resistance. The NMR results suggest that hydroxyl groups within cross-linked silane layers could provide a second pathway for ionic transport based on surface conduction to explain the electrical behavior observed in Figure 1.

Conclusions

Alkylsilane modification of a surface allows the modification of more than the wetting properties. Applied to porous ceramic membranes, alkylsilanes can form multilayers that exclude water from the pores but accommodate ion transport through a surface conduction mechanism. Detailed structural characterization of the alkylsilane layers revealed the presence of hydroxyl groups along the siloxane backbone that act as water wires to accommodate ion transport. This mode of ion transport occurs in shorter-chain alkylsilanes as a result of the higher hydroxyl content in the more extensively cross-linked siloxane backbone. For long-chain alkylsilanes, the ionic transport appears to be dominated by a small number of hydrophilically defective pores.

Acknowledgment. This work was supported by the Nanotechnology Advanced Technology program of GE Global Research. We acknowledge P. Malenfant for help with chemical functionalization, B. Knudsen for assistance with the impedance test cell, E. A. Williams for discussions concerning NMR, H. Hudspeth and R. Rohling for assistance with AAO substrate preparation, L. Denault for SEM imaging, and M. Manoharan and M. Blohm for helpful discussions.

Supporting Information Available: Experimental methods pertaining to the preparation of anodic aluminum oxide supports, Pt electrodeposition, scanning electron microscopy, and air permeability. Characterization of hydrophilically defective pores. Evidence of hydrophilic pore defects via SEM. NMR deconvolution of ^{29}Si spectra and fits from deconvolution. This material is available free of charge via the Internet at http://pubs.acs.org.

LA0615591